Journal of Applied Physics ARTICLE scitation.org/journal/jap

Hydrogen-gas sensing at low concentrations using extremely narrow gap palladium nanoclusters prepared by resistive spectroscopy

Cite as: J. Appl. Phys. **126**, 225104 (2019); doi: 10.1063/1.5119314
Submitted: 10 July 2019 · Accepted: 26 November 2019 ·
Published Online: 11 December 2019

N. Nakamura,[1,a)] T. Ueno,[1] and H. Ogi[2]

AFFILIATIONS

[1]Graduate School of Engineering Science, Osaka University, 1-3 Machikaneyama, Toyonaka, Osaka 560-8531, Japan
[2]Graduate School of Engineering, Osaka University, 2-1 Yamadaoka, Suita, Osaka 565-0871, Japan

[a)]**Electronic mail:** nobutomo@me.es.osaka-u.ac.jp

ABSTRACT

Isolated palladium nanostructures expand when they are exposed to hydrogen gas, and the gaps between them become narrower, thereby decreasing the electrical resistance. This behavior is applicable for the hydrogen-gas sensing, and several types of nanogap structures have been developed. However, the resistance change is significantly small at a low hydrogen-gas concentration because of insignificant lattice expansion. In the present study, this problem is solved by using the palladium nanoclusters with extremely narrow gaps, which is achieved by our original method, resistive spectroscopy, and hydrogen-induced structural stabilization. The nanoclusters are fabricated by interrupting deposition just before forming the continuous film, in which palladium clusters are nearly touching each other, and exposing them to hydrogen gas. In conventional studies using nanoclusters, hydrogen gas is detected through a decrease in the surface electric resistance caused by gap narrowing/closing. However, in this study, we observe an increase in the resistance when the gap distance between the cluster is extremely small, which is attributed to the restriction of electron tunneling between the palladium nanoclusters because of hydrogen adsorption on their surface. We confirm that this mechanism allows ultrahigh sensitivity hydrogen-gas sensing, achieving a limit of detection of 0.25-ppm hydrogen gas. In addition, we find that an optimized structure for the present detection mechanism is different from those in conventional sensors based on the gap-narrowing/closing mechanism.

I. INTRODUCTION

When palladium is exposed to hydrogen gas, the hydrogen-palladium alloy is formed by hydrogen absorption, and it causes lattice expansion.[1] In nanostructures composed of slightly separated palladium clusters, the lattice expansion narrows or closes the gap between the clusters, and it increases the electrical conductivity, because the gap narrowing increases the tunneling (hopping) current and the gap closing changes the conduction mechanism from the tunneling conduction to the bulk conduction. The increase in the conductivity can be more than 100%, and several types of nanostructures have been developed for applying them for hydrogen-gas sensing.[2–10]

The gap-based structures successfully detect hydrogen gas at high concentrations. However, as the hydrogen-gas concentration decreases, the resistive sensitivity to the detection is lowered. Especially, at low concentrations (<100 ppm), the detection becomes difficult, because the lattice expansion is insignificant. This concern should be solved by making the gap as narrow as possible. Ultrathin palladium film[11,12] is a candidate for achieving this. When a metallic material is deposited on a substrate, a continuous film is formed as follows: formation of isolated clusters (island structure), growth of the clusters, and contact between the clusters. Around the transition between the island structure and continuous film, the semicontinuous structure is formed transiently, in which separated and connected clusters coexist and gap distance will be less than 1 nm. Therefore, the gap distance between clusters can be made quite small by interrupting deposition just before the continuous film is formed. However, this morphological change occurs when the film thickness is a few nanometers, and monitoring of the morphological change of such small clusters is difficult, making control of the gap distance difficult. However, in our previous study,[13] we demonstrated that gap distance can be

controlled using resistive spectroscopy, and 100-ppm hydrogen gas was detectable using the semicontinuous films.

In a previous study, we revealed that electrical resistance decreased when the semicontinuous film was exposed to hydrogen gas for the first time.[13] However, it increased in the second and subsequent hydrogen-gas exposures. The change in the hydrogen response indicates that morphology and hydrogen detectability of the semicontinuous film can be controlled by exposing the film to hydrogen gas. In addition, when the gap narrowing/closing occurs only in the first hydrogen-gas exposure, the mechanism cannot be used repeatedly. Therefore, the hydrogen-gas detectability of the semicontinuous film after hydrogen-induced stabilization must be understood.

For these reasons, we investigate the electrical response of the palladium nanoclusters obtained by exposing semicontinuous films to hydrogen gas. As described above, the fabrication of palladium clusters with the desired gap distance is not straightforward. However, we solved this difficulty by developing resistive spectroscopy.[14,15] Using this method, palladium films with different morphologies (discontinuous, semicontinuous, and continuous) are fabricated. Then, their morphology is stabilized by exposing them to hydrogen gas to achieve the extremely narrow-gap (ENG) nanoclusters. We reveal that 0.25-ppm hydrogen gas is detectable using the ENG nanoclusters. In addition, it is found that the optimized morphology observed in this study is different from that observed in the previous study.[13]

II. EXPERIMENTAL

We fabricated the hydrogen-induced stabilized nanoclusters using palladium films fabricated in our previous work.[13] The original films were fabricated by depositing palladium (99.95%) on the silicon substrate (>10 000 Ω cm) using RF magnetron sputtering. The background pressure was less than 2.0×10^{-4} Pa, and argon pressure during deposition was 0.4 Pa. Evolution in the morphology during deposition was monitored using the piezoelectric resonance method.[13] In this method, the piezoelectric material is placed behind the substrate, and palladium is deposited on the top surface of the substrate as shown in Fig. 1(a). During deposition, the attenuation of the resonant vibration of the piezoelectric material is monitored. The vibrating piezoelectric material generates the electric field near the substrate surface, and it causes the electrical current in the deposited palladium, causing Joule heating. Joule heating spends the vibrational energy of the piezoelectric material, and the energy loss changes depending on the morphology (conductivity) of the deposited palladium. In our previous study, we confirmed that the attenuation is at maximum when the semicontinuous film is formed on the substrate; before and after the attenuation maximum, the island structure and continuous structure are formed, respectively.[14,15] Therefore, by monitoring the change in the full-width at half maximum (FWHM) of the resonant spectrum, we can identify the moment of the formation of the semicontinuous film. The piezoelectric material used here is rectangular parallelepiped lithium niobate. The resonant spectrum was measured using the antenna method,[16,17] in which the resonant vibration is excited and the amplitude is measured by generating and detecting electric fields around the piezoelectric material using line antennas. The network analyzer (ZNLE, ROHDE&SCHWARZ) was used for the measurement. The details of the measurement principle and setup are described elsewhere.[14]

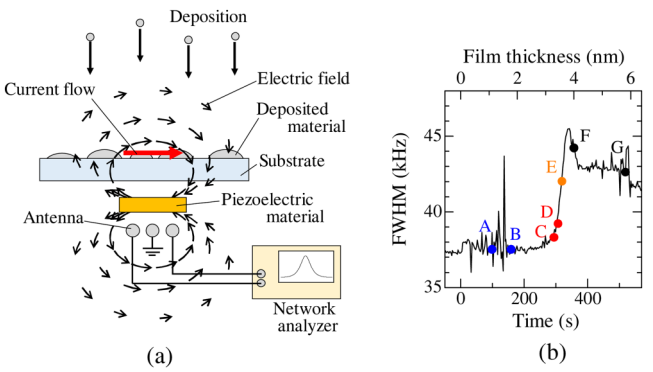

FIG. 1. (a) Schematic image of the simplified measurement setup. (b) Evolution of FWHM during the deposition of film G. Plots denote the moment where deposition was interrupted for preparing the palladium films A–G.

We used seven palladium films, named A–G, which were prepared by interrupting the deposition at different times referring to the change in the FWHM. Figure 1(b) shows the evolution of the FWHM during the deposition of the palladium film G. The appearance of the FWHM peak indicates that the morphological transition occurred around 3.7 nm. In this film, most of the clusters are connected to each other, and there are few isolated clusters. Relative times where the deposition was interrupted for preparing other films are also plotted. Films A and B were prepared by interrupting deposition before the FWHM started to increase. These films are composed of isolated clusters (discontinuous structure). Films C, D, and E were prepared by interrupting the deposition during the FWHM increase. These films are composed of isolated and connected clusters (semicontinuous structure). Film F was prepared by interrupting the deposition during the FWHM decrease. This film also shows the semicontinuous structure, but a large number of clusters are connected to each other compared to the films C–E.

The palladium films were set into the hydrogen-flow cell[13] for hydrogen-induced stabilization and for hydrogen-gas sensing. In the cell, two contacting probes were attached to the film for measuring the surface resistance by the two-terminal sensing. Nitrogen gas was flowed into the cell at a rate of 117 ml/min as a carrier gas. Hydrogen gas with different concentrations in nitrogen was prepared using the autosampler (FLA-1, FDS-1, Shimadzu), and it was added into the carrier gas for hydrogen-gas detection. Its flow rate was 13 ml/min. The total flow rate in the cell was 130 ml/min. As observed in the following experimental results, the resistance was almost stable after hydrogen exposure was finished, which indicates that desorption of hydrogen from palladium barely occurs during nitrogen flow. On a palladium surface covered with oxygen, oxygen is removed by reacting with hydrogen, forming water.[18] In the present study, to remove hydrogen inversely, air in the laboratory was added into the carrier gas, and it was flowed in the cell between each hydrogen exposure. Hydrogen gas and air were flowed for 408 s.

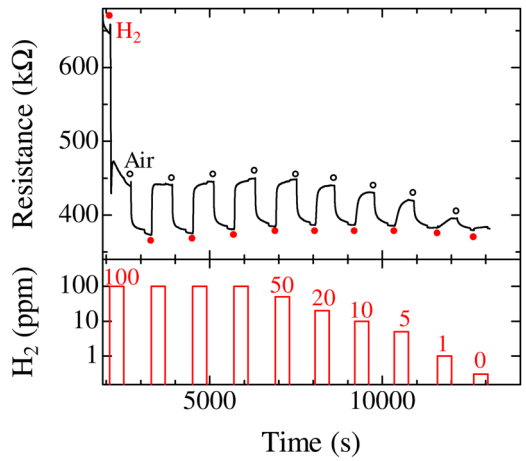

FIG. 2. Electrical resistance of the palladium film D during exposures to hydrogen gas at different concentrations. The top figure shows the electrical resistance, and the bottom figure shows the hydrogen concentration and exposure time. Filled and open circles denote the moment where hydrogen and air were injected, respectively.

III. RESULTS AND DISCUSSION

Figure 2 shows the representative resistance change observed in palladium film D. In the first exposure at 100 ppm, the resistance decreased rapidly. However, the resistance increased in the second and following exposures at 100 ppm. This can be explained by the change in the morphology during hydrogen exposure.[13] When a palladium film composed of separated clusters is exposed to hydrogen, hydrogen absorption causes the volume expansion of the palladium clusters, and some clusters are connected to each other. Once the clusters are connected (percolation happens), they are not detached even after hydrogen is removed. Therefore, in the second and following hydrogen exposures, contact of the clusters does not happen, and resistance does not decrease as observed in the first exposure. The drastic change in the hydrogen response caused by the hydrogen-induced stabilization was observed in the semicontinuous films. Because films B, E, and G had been stabilized in our previous work,[13] in the present study, remaining palladium films were exposed to hydrogen gas at 100 ppm three times for the hydrogen-induced stabilization. After the hydrogen-induced stabilization, the films were exposed to hydrogen gas at 100 ppm and lower concentrations.

Figure 3 shows the changes in the electrical resistance at different hydrogen-gas concentrations for representative three films, A, C, and F. (Full results of these measurements are shown in the supplementary material.) The vertical axis shows the change ratio of the resistance relative to the value R_0 that was measured just before each hydrogen-gas exposure starts. In palladium film A, the resistance increased rapidly, and it gradually decreased at 20, 50, and 100 ppm. At 10 ppm and lower concentrations, the resistance increased monotonically during the hydrogen-gas exposure. Similar behavior was observed in film B. In palladium film C, the resistance increased monotonically at all concentrations, and similar behavior was observed in films D and E. In contrast, the resistance monotonically decreased in the film F. The resistance of the film G also decreased monotonically with time. Thus, the electrical response to hydrogen showed different behaviors, and it was classified into three types, A and B, C–E, and F and G, as described above. In addition, it should be noted that the resistance of the films A–E increased during the hydrogen-gas exposure, whereas the resistance in the conventional gap-based sensors decreases in hydrogen gas. This result indicates that the gap narrowing/closing is not the dominant mechanism of the resistance change in the present films.

The maximum resistance change during the hydrogen-gas exposure is summarized in Fig. 4. Regarding the palladium films A and B, the change ratio increased as the hydrogen-gas concentration increased, but it became almost independent of the hydrogen-gas concentration above 5 ppm. In contrast, the change ratio increased monotonically with the hydrogen concentration in films C, D, and E. Compared to these films, the change ratio of the resistance was small in films F and G.

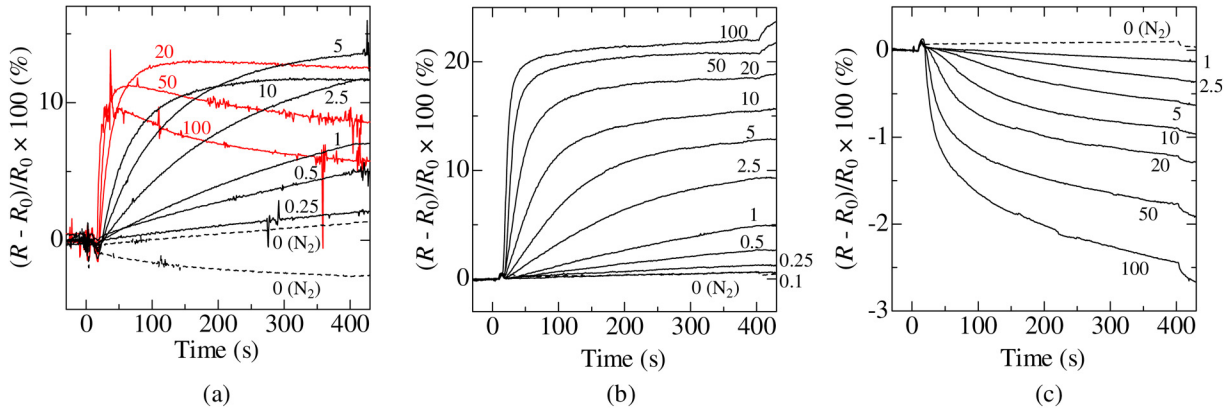

FIG. 3. Evolutions of electrical resistance during hydrogen-gas exposures for palladium film (a) A, (b) C, and (c) F. The number denotes the hydrogen-gas concentration in units of ppm. Dashed curves denote the result when nitrogen gas was flowed. In (b), the dashed curve overlaps with the curve for 0.1-ppm hydrogen flow.

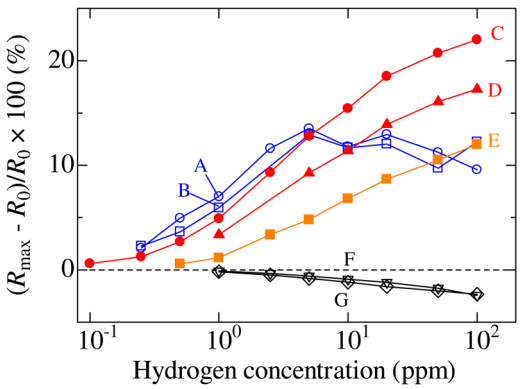

FIG. 4. Maximum change ratio of the electrical resistance during hydrogen-gas exposures.

Regarding films A and B, they are composed of isolated clusters, and their conductivity is governed by the tunneling current as shown in Fig. 5(a). In the films, the resistance changes depending on the gap distance between clusters and work function. When palladium is exposed to hydrogen gas, hydrogen is adsorbed on the palladium surface, and it is then absorbed in the palladium. When hydrogen is adsorbed on the palladium surface, it increases the work function,[19] thereby increasing electrical resistance. In contrast, when hydrogen is absorbed in palladium, the volume increment narrows the gap between clusters, decreasing the resistance. Therefore, it is expected that the resistance first increases due to hydrogen adsorption, and it then decreases by hydrogen absorption. This behavior is observed at 20, 50, and 100 ppm in Fig. 3(a), and it confirms the validity of this interpretation. At lower hydrogen concentrations, a decrease in the resistance was not observed. It is supposed that volume increment by hydrogen absorption barely occurred.

Films C, D, and E are composed of isolated and connected clusters, and the tunneling current still governs the conductivity as shown in Fig. 5(b). In the films, the resistance increases monotonically with time, and the decrease in the resistance was not observed. The change ratio of the resistance was larger than that in films A and B at high concentrations. However, the change ratio decreases as the film thickness (initial electrical conductivity) increases from films C to E. In the first hydrogen exposure (before the hydrogen-induced stabilization), the change ratio of the resistance becomes larger in the film fabricated by interrupting deposition around the FWHM peak.[13] However, after the hydrogen-induced stabilization, the film obtained around the transition between discontinuous and semicontinuous (film C) shows larger electrical response. This indicates that the optimized structure for the tunneling current based sensing is different from that for the gap-narrowing/closing based sensing; the gap distance should be as small as possible for the gap narrowing/closing based sensing, but a larger fraction of isolated clusters is also required for the present sensing mechanism. We consider that the films C and D are composed of such nanoclusters, the ENG nanoclusters, and they show larger resistance change. In film E, the gap distance should be very small, but the fraction of the isolated nanoclusters is small, making the change in the resistance smaller. Therefore, the film is composed of the quasi-ENG nanoclusters.

In films F and G, most of the gaps between clusters are closed in the first hydrogen exposure, and bulk conduction becomes dominant in the second and following exposures [Fig. 5(c)]. In the films, the volume expansion by the hydrogen absorption increases the contacting area between clusters (grain boundaries), and it decreases the electrical resistance. However, the change in the contacting area should be small, and the resistance change was smaller than that observed in other films.

For comparison purpose, experimental results when pure nitrogen gas (0-ppm hydrogen) was flowed instead of hydrogen gas are plotted by dashed lines in Fig. 3. Among the films, film C [Fig. 3(b)] showed the lowest detection limit of 0.25 ppm; the resistance change in nitrogen gas was comparable to that for 0.1 ppm.

Time to reach 90% of the maximum resistance change is plotted in Fig. 6, which is often evaluated as the response time in

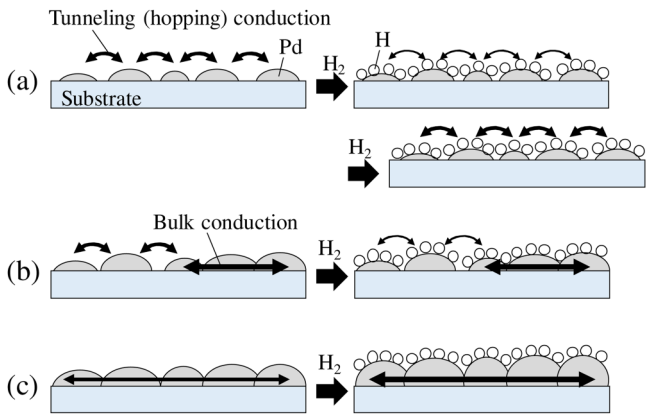

FIG. 5. Schematic images of the film morphology and conduction mechanism of (a) discontinuous, (b) semicontinuous, and (c) continuous film.

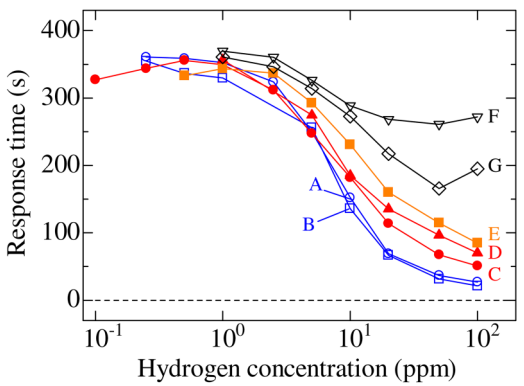

FIG. 6. Response time of the electrical resistance at different hydrogen-gas concentrations.

TABLE I. Comparison of typical hydrogen-gas sensors. Values in parentheses are deduced from the data in the references.

Sensor type	Temperature	Detection limit	Resistance change	Response time	Recovery time
Conductance of ultrathin Pd film[11]	Room temp.	25 ppm	(∼4.5% at 100 ppm)	68 ms at 2% (∼5 s at 100 ppm)	(∼5 s at 2%)
Resistance of Pd thin film[21]	25–100 °C	600 ppm	(∼13% at 1%)	(∼180 s at 1%)	(∼460 s at 1%)
Resistance of Pd nanotube array[20]	Room temp.	100 ppm	247% at 100 ppm	400 s at 100 ppm	(∼1800 s at 100 ppm)
AlGaN/GaN HFET[22]	≥600 °C	10 ppb	…	…	…
Pd/SiO_2/Si MOSFET[23]	150 °C	40 ppm	…	<2 min	…
PdNPs/SiO_2/Si MOS capacitor[24]	Room temp.	1%	…	1.2 s	10 s
Optical fiber with Pt/WO_3[25]	Room temp.	500 ppm	…	10 min at 500 ppm	…
Cantilever[26]	…	≤250 ppm	…	∼5 min	(∼15 min below 0.15%)
Surface acoustic wave[27]	Room temp.	10 ppm	…	20 s	(∼10 min)
Quartz resonator[28]	55 °C	≤1 ppm	…	3–100 s	∼20 min
This work (film C)	Room temp.	0.25 ppm	22% at 100 ppm	51–356 s	∼10 min

previous works.[4,20] In all films, the response time increased as the hydrogen-gas concentration decreased. The response time of the discontinuous film (A and B) was smaller than those of other films. Regarding the recovery time, each hydrogen-gas exposure was started when more than 10 min have passed since the previous exposure was interrupted for films C, D, E, F, and G (the experimental results for films C and F are shown in the supplementary material). In contrast, a recovery time of more than 100 min was needed between hydrogen exposures for films A and B (the experimental result for A is shown in the supplementary material). Thus, the response time of the discontinuous film was smaller than that of other films, but the recovery time was much larger than that of other films. Considering the balance between the response time and recovery time, the semicontinuous film, especially the ENG nanoclusters (films C and D), is suitable for hydrogen sensing.

In Table I, the performance of film C is compared with those of other hydrogen-gas sensors. In the present study, the film C (ENG nanoclusters) showed the largest resistance change, 22%, at 100 ppm, and response time was 51 s. In a previous study using ultrathin palladium films fabricated on self-assembled monolayers,[11] the conductivity change by the gap closing/narrowing mechanism was used, and the conductivity change of ∼4.5% and the response time of about a few seconds were observed at 100 ppm. Compared to this result, the film C shows larger change in the resistance, but the response time is longer. In contrast, the palladium nanotube arrays[20] show the resistance change of 247% at 100 ppm, which is larger than the value obtained in the present study, but the response time is 400 s, which is longer than the value observed in the present study. Using the metal oxide semiconductor field-effect transistor (MOSFET),[23] heterojunction field-effect transistor (HFET),[22] surface acoustic wave,[27] and quartz oscillator,[28] in addition to the above sensors, hydrogen gas at 100 ppm and lower concentrations is detectable. The MOSFET and HFET sensors are generally operated at elevated temperatures to accelerate the response.[29] In contrast, the ENG nanoclusters used in the present study were operated at room temperature. The response time of the ENG nanoclusters will be, therefore, improved by heating them.

IV. CONCLUSIONS

In the present study, we evaluated electrical responses of palladium films with different morphologies to hydrogen gas at 100 ppm and lower concentrations. We revealed that, in discontinuous and semicontinuous films, the electrical resistance increased in hydrogen gas, and 0.25-ppm hydrogen gas was detectable using the ENG nanoclusters. In the conventional hydrogen-gas sensing using nanogap structures, hydrogen gas was detected using gap narrowing/closing. However, in the discontinuous and semicontinuous films used in the present study, the change in the work function by hydrogen adsorption was used for the hydrogen-gas sensing, and the applicability of the ENG nanoclusters to hydrogen-gas sensing at low concentrations was demonstrated.

SUPPLEMENTARY MATERIAL

See the supplementary material for full data of experimental results in Fig. 3.

ACKNOWLEDGMENTS

This research was partially supported by the JSPS KAKENHI (Grant No. 18H01883). A part of this study was also supported by the Development of Advanced Measurement and Analysis Systems from theJapan Science and Technology Agency (JST).

REFERENCES

[1]T. B. Flanagan and W. A. Oates, Annu. Rev. Mater. Sci. **21**, 269–304 (1991).
[2]F. Favier, E. C. Walter, M. P. Zach, T. Benter, and R. M. Penner, Science **293**, 2227–2231 (2001).
[3]T. Kiefer, F. Favier, O. Vazquez-Mena, G. Villanueva, and J. Brugger, Nanotechnology **19**, 125502 (2008).
[4]B. Xie, L. Liu, X. Peng, Y. Zhang, Q. Xu, M. Zheng, T. Takiya, and M. Han, J. Phys. Chem. C **115**, 16161–16166 (2011).
[5]J. Lee, W. Shim, E. Lee, J. Noh, and W. Lee, Angew. Chem. Int. Ed. **50**, 5301–5305 (2011).
[6]M. Zhao, M. H. Wong, and C. W. Ong, Appl. Phys. Lett. **107**, 033108 (2015).
[7]G. Kaltenpoth, P. Schnable, E. Menke, E. C. Walter, M. Grunze, and R. M. Penner, Anal. Chem. **75**, 4756–4765 (2003).

[8]M. Zhao, M. H. Wong, C. W. Ong, N. H. Ng, and H. C. Man, Sens. Actuators B **255**, 944 (2018).
[9]Q. Zhao, J. Shao, H. Tian, X. Li, C. Wang, and J. Liu, Sens. Actuators B **270**, 475–481 (2018).
[10]X. Li, T. Cao, X. Zhang, Y. Sang, L. Yang, T. Wang, Y. Li, L. Zhang, L. Guo, and Y. Fu, Sens. Actuators B **295**, 101–109 (2019).
[11]T. Xu, M. P. Zach, Z. L. Xiao, D. Rosenmann, U. Welp, W. K. Kwok, and G. W. Crabtree, Appl. Phys. Lett. **86**, 203104 (2005).
[12]T. Kiefer, L. G. Villanueva, F. Fargier, F. Favier, and J. Brugger, Appl. Phys. Lett. **97**, 121911 (2010).
[13]N. Nakamura, T. Ueno, and H. Ogi, Appl. Phys. Lett. **114**, 201901 (2019).
[14]N. Nakamura and H. Ogi, Appl. Phys. Lett. **111**, 101902 (2017).
[15]N. Nakamura, N. Yoshimura, H. Ogi, and H. Ogi, J. Appl. Phys. **118**, 085302 (2015).
[16]H. Ogi, K. Motohisa, T. Matsumoto, K. Hatanaka, and M. Hirao, Anal. Chem. **78**, 6903–6909 (2006).
[17]N. Nakamura, M. Sakamoto, H. Ogi, and M. Hirao, Rev. Sci. Instrum. **83**, 073901 (2012).
[18]D. Gupta, D. Dutta, M. Kumar, P. B. Barman, C. K. Sarkar, S. Basu, and S. K. Hazra, Sens. Actuators B **196**, 215–222 (2014).
[19]H. Conrad, G. Ertl, and E. E. Latta, Surf. Sci. **41**, 435–446 (1974).
[20]M. A. Lim, D. H. Kim, C. O. Park, Y. W. Lee, S. W. Han, Z. Li, R. S. Williams, and I. Park, ACS Nano **6**, 598–608 (2012).
[21]S. Öztürk and N. Kılınç, J. Alloys Compd. **674**, 179–184 (2016).
[22]J. Song and W. Lu, IEEE Electron Device Lett. **29**, 1193–1195 (2008).
[23]I. Lundström, S. Shivaraman, C. Svensson, and L. Lundkvist, Appl. Phys. Lett. **26**, 55–57 (1975).
[24]G. Behzadi pour and L. Fekri aval, Results Phys. **7**, 1993–1999 (2017).
[25]Z. Li, M. Yang, J. Dai, G. Wang, C. Huang, J. Tang, W. Hu, H. Song, and P. Huang, Sens. Actuators B **206**, 564–569 (2015).
[26]S. J. McKeown, X. Wang, X. Yu, and L. L. Gddard, Microsyst. Nanoeng. **3**, 16087 (2017).
[27]K. Yamanaka, S. Ishikawa, N. Nakaso, N. Takeda, D. Y. Sim, T. Mihara, A. Mizukami, I. Satoh, S. Akao, and Y. Tsukahara, IEEE Trans. Ultrason. Ferroelectr. Freq. Control **53**, 793–801 (2006).
[28]L. Zhou, N. Nakamura, A. Nagakubo, and H. Ogi, Appl. Phys. Lett. **115**, 171901 (2019).
[29]T. Hübert, L. Boon-Brett, G. Black, and U. Banach, Sens. Actuators B **157**, 329–352 (2011).